Research Square

Preprints are preliminary reports that have not undergone peer review.
They should not be considered conclusive, used to inform clinical practice,
or referenced by the media as validated information.

Response and mechanism on the growth dynamics of mulberry seedlings to calcium under drought stress

Haoyan Liu
Shenyang Agricultural University
Tengzi Zhang
Shenyang Agricultural University
Zhen Wang
Dalian University
Qingqing Cui
Dalian University
Siyu Zuo
Dalian University
Chengshu Xin
Dalian University
Qing Yu
Dalian University
Zhi Song
Dalian University
Liwei Chu
chuliwei@dlu.edu.cn
Dalian University
Yongbin Zhou
Dalian University

Research Article

Keywords: Drought stress, Calcium heterogeneity, Photosynthesis, Transcriptomics, Metabolomics, WGCNA

Posted Date: June 24th, 2026

DOI: https://doi.org/10.21203/rs.3.rs-9812354/v1

License: This work is licensed under a Creative Commons Attribution 4.0 International License.
Read Full License

Abstract

In arid and semi-arid regions, calcium, a heterogeneous element, along with water, affects plant growth. Mulberry (Morus alba L.) is a significant ecological and economic forest species in semi-arid regions. To investigate the effects of Ca addition on the physiological indicators of mulberry seedlings under drought stress, this experiment was set up with water treatments (normal water supply: 70±5% of the maximum water holding capacity; drought stress: 40±5% of the maximum water holding capacity) and Ca addition (Ca0:0 mg·kg-1 Ca2+; Ca400:400 mg·kg-1 Ca2+) two factors. Sampling was carried out five times (S1, S2, S3, S4, and S5) in the two-year growing season of mulberry seedlings for physiological indicators, and S2 for transcriptome and metabolome analyses were performed on the leaves of mulberry seedlings treated with Ca0 and Ca400 under normal water supply conditions and Ca400 under drought stress. Comparative transcriptomic analysis revealed that the differentially expressed genes (DEGs) between Ca400-DC and Ca0-DC were significantly enriched in flavonoid biosynthesis and carotenoid metabolism pathways. The upregulation of 20 key photosynthetic genes in Ca400 inhibited drought. The downregulation of 20 PSI and PSII light-harvesting protein-related genes and 16 downregulation of genes related to subunits on PSI and PSII severely inhibited the photosynthetic ability of mulberry seedlings. Using weighted gene co-expression network analysis (WGCNA), seven candidate genes were identified from eight modules that were highly correlated with phenylpropanoid synthesis in mulberry leaves. These genes may play key regulatory roles in mulberry and could serve as candidate genetic resources for preventing drought. Additionally, three important metabolic pathways were observed in the metabolomics analysis: the phenylpropanoid biosynthesis pathway, photosynthesis pathway, and antenna protein pathway. This study deepens our understanding of the adaptive responses of mulberry seedlings to drought-Ca heterogeneity and provides theoretical guidance for mulberry afforestation and forest management in semi-arid areas.

1. Introduction

Drought is a major environmental factor affecting plant survival, and the occurrence of drought in forest ecosystems has received extensive attention from the scientific community because of its increasing frequency (Duursma et al., 2008; Murray and Ebi, 2012; Williams et al., 2013; Aaltonen et al., 2016; Yu and Zhai, 2020). Extreme droughts affect plant physiological functions, growth (Yang et al., 2023), productivity, and mortality. Drought has caused many large-scale forest die-offs over the past century (Hartmann et al., 2018), and in recent years, rising global temperatures have amplified the changes in forests caused by drought. Revealing the mechanisms by which plants respond to drought stress is of critical importance for predicting plant growth and development under future climate change conditions (Xu et al., 2019; Hammond et al., 2022).

Calcium (Ca) is an essential mineral nutrient for plant growth and development, and as a cellular structural substance and second messenger, it has a significant impact on all aspects of plant growth and development (Li et al., 2010). As one of the bulk nutrients in plants, plants mainly take up calcium via the exoplasmic pathway and transport it to various meristematic tissues through transpiration

gravitational force for growth or to form insoluble and stable compounds (e.g., calcium oxalate), with little redistribution and transport (Jing et al., 2013). Therefore, plants require a continuous supply of calcium during growth and have a limited ability to compensate for calcium deficiency or excess in tissues. Differences in soil calcium supply reflect the amount of calcium absorbed by plants, particularly the concentration of calcium in neoplastic tissues (Li et al., 2021). In recent years, with the in-depth study of calcium, the role of calcium in plant growth has received increasing attention, and both calcium deficiency and excess can inhibit plant growth. Previous studies have found peach trees and found that calcium deficiency inhibits plant growth, disrupts cell membrane structure, and inhibits chlorophyll biosynthesis (Aras et al., 2021). Some researchers have found that calcium deficiency led to a decline in the photosynthetic rate, biomass accumulation, and reduction in the nutrient absorption capacity of poplars (Weng et al., 2022). The nutrient uptake capacity was reduced. Under conditions of plant calcium deficiency, exogenous calcium addition can alleviate the inhibitory effects suffered by plants. For example, calcium carbonate and calcium silicate can improve soil quality and plant productivity (Gradowski and Thomas, 2008; Kang et al., 2017). Excess calcium can lead to stomatal closure of plant leaves, suppressing the photosynthetic and growth rates of plants (Li et al., 2022). In addition, excess Ca^{2+} in cells can form precipitates with PO_4^{3-}, which can interfere with processes related to phosphorus metabolism, impede normal signaling, and affect plant growth (Ji Feiteng et al., 2009).

Mulberry (*Morus alba* L.) is an important perennial economic tree species with a wide ecological distribution (Rohela et al., 2020a). In recent years, mulberry has been recognized as a multipurpose plant, and in addition to its use in the mulberry sericulture industry, mulberry leaves have been used in feed processing and food health care. (Chao et al., 2021; Liu et al., 2022). Mulberry also has important ecological value, and its role in ecological management, such as soil and water conservation, wind and sand control, greening of barren mountains, and remediation of polluted sites, has been gradually emphasized (Liu et al., 2021). In addition, mulberries can purify the air by sequestering carbon, which plays an important role in protecting the environment and is classified as a sustainable development plant (Rohela et al., 2020b). Mulberry trees are more adaptable to harsh natural environments, showing tolerance to salt, drought, cold, waterlogging, and heavy metal ions (He et al., 2012; Zhang et al., 2020b). However, they still suffer from abiotic and biotic stresses that adversely affect their growth and productivity.

Most current studies on mulberry under drought stress remain at the physiological and biochemical levels, and there is still little research on the molecular mechanisms of drought resistance in mulberry.

In this study, physiological profiling of mulberry at different stages and under different water and Ca conditions revealed that S2 stage mulberry seedings have obvious changes. Through transcriptome analysis, we identified key DEGs in the phenylpropanoid synthesis and photosynthesis pathways. Furthermore, weighted gene co-expression network analysis (WGCNA) highlighted seven candidate genes as potential regulators of photosynthesis. These findings establish a molecular framework for elucidating the adaptive responses of mulberry seedlings to drought-Ca heterogeneity and provide theoretical guidance for mulberry afforestation and forest management in semi-arid areas.

2. Materials and Methods

2.1 Plant materials and experiment design

The experiment was set up in a greenhouse at the base of the mountain at Shenyang Agricultural University (41°48'11.75"N123°25'31.18"E). In each growing season, the average temperature of the greenhouse was 25±2 °C and the average relative humidity was 60%. The test soil was a windy sandy soil with a pH6 of.75, organic carbon of 6.46 g•kg^{-1}, total nitrogen of 0.58 g•kg^{-1}, total phosphorus of 0.07 g•kg^{-1}, and water-soluble calcium of 0.02g•kg^{-1}. This study selected sandy soils with extremely low water-soluble calcium content to better simulate soil calcium heterogeneity—that is, varying levels of soil calcium—in arid and semi-arid regions.

The mulberries (*Morus alba* L.) were a drought-resistant asexual line, Arxiang, selected from the experimental base of Shenyang Agricultural University in Fuxin City, Liaoning Province, China. All mulberry seedlings were grown in pots for one month to adapt to the environment, ensuring survival—acclimatization (bottom diameter: 18.3 cm; outer diameter: 22.5 cm; height: 21.5 cm), and calcium addition and drought treatment were started when the seedlings were approximately 8 cm tall. To prevent the introduction of exogenous calcium from tap water, deionized water was used to maintain soil moisture throughout the process.

The three treatments were normal water supply (70±5% of the maximum water holding capacity, Ca0-MC), drought treatment (40±5% of the maximum water holding capacity, Ca0-DC), and calcium addition in drought treatment (400 mg·kg^{-1} Ca^{2+} addition in 40±5% of the maximum water holding capacity, Ca400-DC), with 45 pots for each treatment. Soil moisture (40%) was maintained through daily weighing of the pots.

Calcium was added to the soil as an aqueous calcium chloride solution. After calcium addition, water control was initiated when the soil moisture content was reduced to the target water level (40±5% of the maximum holding capacity) and rehydrated every 1 d.

The experimental design, analysis of results, and discussion throughout the paper revolve closely around the core variable of “calcium supplementation.” The aim is to investigate the role of “calcium” (Ca^{2+}) under drought stress. All interpretations point to the effects of calcium ions (Ca^{2+}). The entire explanatory logic is built on the premise that “calcium ions” are the primary causative factor. This data-supported, self-consistent “calcium-centric” explanatory framework may lead us to believe that there is no need to introduce another variable—Cl^- toxicity—that has not been directly verified by this study to provide a relatively more complex attribution.

Destructive sampling was conducted on June 10, 2020 (S1 stage, early growth), August 20, 2020 (S2 stage, fast-growing period), September 25, 2020 (S3 stage, end of growth), June 15, 2021 (S4 stage, early growth), and August 25, 2021 (S5 stage, fast-growing), with six pots taken from each treatment.

2.2 Individual morphometry

The dry masses of the roots, stems, and leaves of the mulberry trees were determined using an analytical balance (BSA124S, Sartorius, Germany), and the mass fraction of each organ was calculated as the biomass of each organ divided by the total biomass.

Leaf area: Before each sampling, leaf area was scanned with a hand-held leaf area meter (CI2-203), and three representative leaves from different parts of each plant were selected; the three leaves were dried and weighed to calculate the specific leaf area. The specific leaf area was calculated as the ratio of leaf area to leaf biomass.

Root morphology (WinRHIZO Root System Analysis Software): primary root length, total root length, total root surface area, root volume; specific root length was calculated as the ratio of total root length to root biomass.

2.3 Measurement of photosynthetic and fluorescence parameters

Before each sampling, a sunny morning was selected, at 8:00-11:00 a.m. using a Li-6400 (LI-6400XT, LICOR Biosciences, Lincoln, NE, USA) portable photosynthesis assay system and a red and blue light source 6400-02 (LI-6400XT, LI-COR Biosciences, Lincoln, NE, USA), the first fully expanded leaf of the same length was selected for the measurement; the photosynthetic parameters such as net photosynthetic rate (Pn), stomatal conductance (Gs), and transpiration rate (Tr) of mulberry seedling leaves were recorded in six replications for each treatment. The instantaneous water-use efficiency (WUE) was calculated as WUE=Pn/Tr. We measured the fluorescence parameters using a portable pulse-modulated chlorophyll fluorometer (Opti-Sciences OS-5p+). Six replicates were used for each treatment, and the average value was calculated. Before measurement, the mulberry leaves were dark-treated for 30 min. The ecological significance of the fluorescence indicators is presented in Supplementary Table 1.

2.4 Transcriptome sampling

After the S2 stage, mulberry seedling samples' leaves were collected under three treatment conditions for transcriptome sequencing: Ca0 treatment under normal watering conditions, and Ca0 and Ca400 treatments under drought stress. For each treatment, 3 replicates were taken. From each mulberry seedling, 9 fully matured leaves from top to bottom were collected, wrapped in tin foil, and placed in a resealable bag, rapidly frozen in liquid nitrogen, and stored at -80°C.

2.5 RNA extraction, libraries construction, and sequencing

Total RNA was extracted from the samples using the Trizol method, following the instructions for the Plant Total RNA Extraction Kit (TIANGEN BIOTECH (BEIJING) CO., LTD). The integrity and quantity of the RNA were measured using an Agilent 2100 bioanalyzer. The library was constructed using total RNA. First, qualified total RNA samples were enriched with mRNA with polyA tails using Oligo(dT) magnetic beads. The enriched mRNA was then randomly fragmented and used as a template to synthesize the first strand of cDNA with random oligonucleotide primers in an M-MuLV reverse transcriptase system. Subsequently, the RNA strand was degraded with RNaseH, and the second strand of cDNA was synthesized with DNA polymerase I using dNTPs as substrates. The purified double-stranded cDNA underwent end repair, addition of an A-tail, and ligation with the sequencing adapters. cDNA fragments of approximately 370–420 bp were selected, PCR-amplified, and purified again to obtain the final library. After quality control, different libraries were pooled according to the effective concentration and targeted sequencing data volume and then sequenced on the Illumina platform.

2.6 Differential Expression Gene Screening and GO and KEGG enrichment analysis

Fragments Per Kilobase Million (FPKM) values were used to indicate the expression abundance of the corresponding unigenes. The degeR package was used for differential expression analysis between different pairs of comparisons. Benjamini-Hochberg method was used to select the different pairs of Unigenes with FDR less than 0.05 and fold FC greater than or equal to 1.5 and FDR less than 0.01 and fold FC greater than or equal to 2.0. were used as screening criteria. Functional annotation of differentially expressed genes was performed using KEGG databases, and enrichment analysis was performed based on the annotation results.

2.7 Target gene qRT-PCR validation

Based on the transcriptional sequencing data, GAPDH was selected as a candidate gene for validation according to the physiological responses of the mulberry seedlings to drought stress and calcium addition. Primers were designed using Primer-BLAST, and the primer sequences are shown in Supplementary Table 2. GAPDH was selected based on transcriptomic sequencing data and the physiological responses of mulberry seedlings to drought and calcium supplementation. Our preliminary analysis of the transcriptomic data indicated that GAPDH expression remained relatively stable across different treatments, leading to its selection as a candidate internal control gene.

2.8 Metabolite extraction and chromatographic analysis

Metabolite Extraction: Accurately weigh 100 mg of leaf samples that have been ground in liquid nitrogen. Add 500 µL of an 80% methanol-water solution, vortex to mix, and incubate on an ice bath for 5 minutes. Centrifuge at 4°C and 15,000 x g for 20 minutes. Take a certain volume of the supernatant, dilute it with

mass spectrometry-grade water to a methanol concentration of 53%, and centrifuge again under the same conditions. The resulting supernatant is used for LC-MS analysis.

Chromatographic Conditions: Separation was performed using a Thermo Fisher Hypesil Gold column (100 × 2.1 mm, 1.9 μm) at a column temperature of 40°C and a flow rate of 0.2 mL/min. In positive ion mode, mobile phase A was 0.1% formic acid in water, and mobile phase B was methanol; in negative ion mode, mobile phase A was 5 mM ammonium acetate in water at pH 9.0, and mobile phase B was methanol. (Supplementary Table 3).

2.9 Differential Metabolite Screening and KEGG Enrichment

A combination of differential multiplicity and VIP values from the OPLS-DA model was adopted to screen for differential metabolites, and the screening criteria were FC>2.0, VIP>1.0. Functional annotation of the differential metabolites was performed using the KEGG database, and KEGG pathway enrichment was performed based on the annotation results.

2.10 WGCNA

A gene co-expression network was constructed using R software (version 4.3.1) and the WGCNA package (version 1.72) with default parameters. The goodSamplesGenes function was used to filter out Samples Genes with missing values or outliers. Hierarchical clustering analysis was performed using the hclust package to cluster the samples and remove outliers. The soft-thresholding power for network construction was determined based on the scale-free topology criterion (R^2 > 0.9) using Fragments Per Kilobase Million (FPKM) values of all genes across samples. The correlation between the modules and the four pigment contents was determined by estimating the module-trait relationship, and KEGG enrichment and GO annotation analyses were performed on all modules using the Omicshare platform (https://www. omics hare. com/).

2.12 Data processing

Data were statistically analyzed using SPSS 26.0 (SPSS, Inc., Chicago, IL, USA). A two-way ANOVA was used to analyze the effects of drought stress and calcium addition on mulberry seedling growth, biomass accumulation and partitioning, tissue morphology, and photosynthetic characteristics at different growth stages. One-way ANOVA was used for the analysis of variance, and Duncan's multiple comparisons were used to analyze the differences between different treatments at the same sampling time (p<0.05). Principal component analysis (PCA) was performed using the built-in statistical function prcomp in R software (https://www.r project.org). Cluster heatmap and Pearson's correlation coefficient

were plotted using the Complex Heatmap toolkit of R. Excel 2016 was used for table plotting, and Origin 2021 was used for bar chart and radar plotting.

3. Results

3.1 Response of mulberry seedling tissue morphology to calcium addition under drought stress

Drought significantly reduced the plant height, diameter, stem biomass, leaf area, and leaf biomass of mulberry seedlings at all stages (*p<0.05)*. Calcium addition further inhibited the increase in mulberry seedling plant height, diameter, stem biomass, leaf area, and leaf biomass during the S2 stage (Figure 1A–E; Supplementary Table 4-5; Supplementary Table 7).

Under normal water supply conditions, main root length, lateral root length, root surface area, root volume, main root biomass, and lateral root biomass significantly increased from S1 to S5 ($p<0.05$). During the S2 stage, drought stress significantly decreased the main root length, lateral root length, root surface area, and root volume and calcium addition significantly exacerbated this situation (Figure 1 F-L; Supplementary Table 6-7).

3.2 Photosynthetic physiological response mechanism of mulberry seedlings to calcium addition under drought stress

Drought significantly reduced Pn, Gs, Tr, WUE, V_j, Fm, Mo, and PIabs in mulberry seedlings at all stages (*p<0.05*). Calcium addition further decreases the Pn, Gs, Tr, and PIabs from S1 to S3, but further increases from S3 to S5 (Figure 2A-H; Supplementary Table 9).

Under normal water supply conditions, Pn, Gs, and Tr significantly decreased from S1 to S3 and significantly increased from S3 to S5 ($p<0.05$). During the S2 stage, all three treatments showed significant decreases, and drought stress significantly decreased Pn, Gs, Tr, WUE, V_j, Fm, Mo, and PIabs, and calcium addition significantly exacerbated this situation (Figure 2 A-H; Supplementary Table 9).

Drought significantly influenced the ABS/RC, ETo/RC, DIo/RC, RC/CS, DIo/CS, ABS/CS, and φPo of mulberry seedlings at all stages (*p<0.05)*. Calcium addition further influenced the ABS/RC, DIo/RC, and RC/CS of the mulberry seedlings (Figure 3A-E; Supplementary Table 10-11). The S2 period showed a significant influence in all periods and all three treatments.

Under normal water supply conditions, ABS/RC, TRo/RC, DIo/RC, RC/CS, ETo/CS, DIo/CS, ABS/CS, ψEo, φEo, ψPo, φPo, δRo, and φRo increased significantly from S1 to S5 ($p<0.05$). Drought stress significantly decreased the main ABS/RC and calcium addition significantly exacerbated this situation (Figure 3 A-E;

Supplementary Table 10-11). The S2 period showed a significant influence in all periods and all three treatments.

3.3 RNA Sequencing results and DEG analysis of mulberry seedlings in response to calcium addition under drought stress

Our study found that S2 stage mulberry seedlings showed significant changes in photosynthetic parameters, biomass accumulation, and root morphology. Sampling at this stage can reveal the molecular mechanisms underlying phenotypic changes using histological data. Therefore, after careful consideration, we chose the sample at the S2 over other periods for transcriptome, metabolome, and WGCNA determination.

Transcriptome analysis of 9 mulberry seedling leaf samples was completed using RNA-Seq technology. A total of 82.26 Gb of clean data were obtained. The clean data of all samples reached 6.25 Gb, the percentage of Q20 bases reached over 97%, the percentage of Q30 bases reached over 92%, and the GC content was over 45%, which indicated that the sequencing results were reliable and could be analyzed in the next step (Supplementary Table 12). The correlation of gene expression levels among samples is an important index for testing the reliability of the experiment and the reasonableness of sample selection. In this study, the R^2 between the biological replicates was between 0.80 and 0.956, indicating that the data were reliable and the sample selection was reasonable (Supplementary Figure 2).

The differential gene expression among the different comparison groups was obtained through screening, and the clustering heat map results showed significant differences in gene expression among the treatments (Supplementary Figure 3A-B). By analyzing the expression of differential genes among the comparison groups, it was found that the Ca400-DC comparison group had the most differentially expressed genes, totaling 8356 genes, 4065 upregulated genes, and 4291 downregulated genes. The Ca0-MC group had the fewest number of differentially expressed genes, with 2198 genes, 971 upregulated genes, and 1227 downregulated genes. In the Ca0-DC comparison group, there were 3253 differentially expressed genes, 1521 upregulated genes, and 1732 downregulated genes.

According to the results of the preliminary stage of this experiment, 10 genes related to the physiological and biochemical indices of mulberry seedlings in response to drought stress and Ca400 were selected for qRT-PCR, and the relative expression levels of the 10 genes were calculated using GAPDH as the internal reference. A linear correlation analysis was carried out between the transcriptome differentially expressed folds and qRT-PCR (Supplementary Figure 4), and the correlation coefficient was 0.961, which indicated that the correlation was better, and the transcriptome sequencing data were more accurate, so that the transcriptome data can be related to the analysis of the transcriptome data.

3.4 KEGG of mulberry seedlings in response to calcium addition under drought stress for DEGs

KEGG functional annotation and analysis of the annotated differential genes demonstrated that the significance was in the top 20 metabolic pathways (Figure 4A-C). Under drought stress (Ca0-DC), the ten most enriched pathways were starch and sucrose metabolism, protein processing in the endoplasmic reticulum, plant-pathogen interaction, pentose and glucuronate interconversions, phenylpropanoid biosynthesis, flavonoid biosynthesis, photosynthesis, photosynthesis-antenna proteins, amino sugar and nucleotide sugar metabolism, and plant hormone signal transduction.

Ca400 treatment under drought stress (Ca400-DC), the 13 most enriched pathways were urea and other terpenoid-quinone biosynthesis, hormone signaling, phenylpropanoid metabolism, carbon fixation in photosynthetic organisms, circadian rhythms in plants, flavonoid biosynthesis, photosynthesis-antenna, fructose and mannose metabolism, galactose metabolism, glycolysis/glyconeogenesis pathway, starch and sucrose metabolism pathway, photosynthesis pathway, and amino and nucleotide sugar metabolism pathway.

3.5 Phenylpropanoid Metabolic Process of mulberry seedlings in response to calcium addition under drought stress

This study investigated the processes of phenylpropanoid biosynthesis and metabolism, with 36 DEGs encoding seven types of bio-enzymes (Figure 5). Under drought stress (Ca0-DC), three upregulated genes were annotated as flavonol synthase (FLS), one upregulated gene was annotated as flavonoid 3'-monooxygenase (CYP75B1), and one upregulated gene was annotated as bifunctional dihydroflavonol 4-reductase/flavanone 4-reductase (DFR). 1 upregulated gene was annotated as flavonoid 3'-monooxygenase (CYP75B1) in the Ca400 treatment (Ca400-DC) under drought stress. In addition, the phenylalanine, spermidine, trans-cinnamic acid, erucic acid, erucinol, pinacoside, eugenol methyl ester, and eugenol methyl ester contents increased after drought stress Ca400 treatment. The levels of and eugenol methyl ether increased, while those of coumarin and scopolamine decreased under drought stress Ca400.

3.6 Photosynthesis pathways of mulberry seedlings in response to calcium addition under drought stress

In the photosynthesis section, the antenna protein and photosynthesis pathways (Figure 6) were identified. Under drought stress (Ca0-DC), 2 downregulated genes were enriched for the photosynthetic antenna protein pathway, annotated as light-trapping pigment complex II chlorophyll a/b binding protein

1 (Lhcb1). The photosynthesis pathway was enriched with 3 downregulated differentially expressed genes, 1 gene annotated as plastidial blue light (petE), and 2 genes annotated as subunit XI (psaL) and subunit PsaN (psaN) of photosystem I.

In the Ca400 treatment under drought stress (Ca400-DC), 20 downregulated differential genes in the antenna protein pathway, 11 of which were annotated as chlorophyll a/b binding protein of light-trapping pigment complex I (Lhca), and 9 of which were annotated as chlorophyll a/b binding protein of light-trapping pigment complex II (Lhcb) in the photosynthesis pathway. The major differential genes enriched in the photosynthesis pathway were 18 downregulated genes, 2 upregulated genes, and 1 downregulated differential metabolite, ATP; 2 upregulated genes were annotated as photosystem II CP43 chlorophyll deconjugated proteins (psbC), 3 downregulated genes as photosystem II oxygen-enhancing proteins (OEPs), 1 downregulated gene as a photosystem II 22 kDa protein (psbS), 1 downregulated gene as a photosystem II PsbY protein (psbY), and 1 downregulated gene was annotated to photosystem II Psb27 protein (psb27). 1 downregulated gene was annotated as a photosystem II 13kDa protein (psb28), 8 downregulated genes were annotated as photosystem I subunits, 1 downregulated gene was annotated as plastocyanin (petE), 1 downregulated gene was annotated as an iron redox protein (petF), and 1 downregulated gene was annotated as an F-type H^+ transporter ATPase γ subunit.

In summary, drought stress inhibits various physiological and biochemical processes in chloroplasts, including photosynthetic pigments, photosystems, primary reactions, photosynthetic electron transport, and carbon fixation.

3.7 Metabolic pathway and metabolite correlation analysis of mulberry seedlings in response to calcium addition under drought stress

The quality control (QC) samples exhibited minimal dispersion in the analytical data, confirming instrument stability and data reliability. Principal component analysis (PCA) revealed clear separation among the four treatment groups, with principal component 1 (PC1) and principal component 2 (PC2) accounting for 38.38% and 21.33% of the total variance, respectively. Biological replicates clustered tightly, demonstrating high reproducibility (Supplementary Figure 5).

Under drought stress alone (Ca0-DC), the most significantly upregulated pathways included amino acid biosynthesis (particularly arginine biosynthesis), purine metabolism, flavone and flavonol biosynthesis, carbon fixation in photosynthetic organisms, and carotenoid biosynthesis. Under drought stress (Ca400-DC), the metabolites that accumulated the most were secondary metabolites, amino acids, phenylpropanoids, phenylalanine, tryptophan, carbon fixation in photosynthetic organisms, isoflavones, carbon, aminoacyl-tRNA, cysteine and methionine, glycolysis, carotenoids, pyruvate, photosynthesis, and porphyrin and chlorophyll. By grouping metabolites under different treatments, Ca0-DC detected the fewest differential metabolites, with 361 differential metabolites, 179 upregulated metabolites, and 182

downregulated metabolites, and the difference in the number of upregulated and downregulated metabolites was not significant (Supplementary Figure 6). A total of 468 differential metabolites were detected in Ca0-MC, including 253 upregulated and 215 downregulated metabolites. Ca400-DC detected the highest number of differential metabolites (713). A total of 419 upregulated and 294 downregulated metabolites were identified (Supplementary Figure 7).

3.8 Detection of Correlations among Gene Modules and Metabolite Traits via WGCNA Analysis

To reveal the relationships between genes and metabolic pathways and identify new pathways contributing to the construction of metabolic networks, 20 metabolic pathways were selected for weighted gene co-expression network analysis (WGCNA). Higher correlations were observed between the modules and several compounds (Figure 8A). Two modules were selected for the KEGG enrichment analysis (Figure 8B–E).

The blue module had high correlation values with guanosine 5'-diphosphate, lumichrome, and D-ribulose 5-phosphate, with values of 0.51, 0.52, and 0.52, respectively (Figure 8A). The first, second, and third most enriched pathways were RNA transport, riboflavin metabolism, and endocytosis, respectively (Figure 8B), indicating potential links between metabolites and these pathways.

The black module was correlated with prostaglandin H2, arachidonic acid, and thromboxane B2, with correlation values of 0.49, 0.48, and 0.5, respectively (Figure 8A). KEGG enrichment analysis showed that genes were processed in the arachidonic acid metabolism, glyoxylate and dicarboxylate metabolism (Figure 8C), providing evidence for gene regulation of prostaglandin H2, arachidonic acid, and thromboxane B2 reduction in mulberry seedlings under different calcium treatment and drought stress.

To identify the potential key genes involved in regulating the complex networks under different calcium treatment and drought stress, we gathered the hub genes for each module according to their connectivity (also called degree). The hub genes for the blue and black were LOC21391025 (delta-1-pyrroline-5-carboxylate dehydrogenase 12A1), LOC21391362 (UDP-glycosyltransferase 92A1), LOC21393691(glycosyltransferase), LOC21397608(U-box domain-containing protein 12), LOC21404943(ras-related protein RABH1e), LOC21406890(uncharacterized protein), LOC21387191(vacuolar-sortingreceptor3), LOC21395038(sister chromatid cohesion 1 protein 4), LOC21407567(1,4-alpha-glucan-branching enzyme 1, chloroplastic/amyloplastic), LOC21403099(UDP-galactose transporter 1).

Ninety upregulated DEGs were possibly connected to the hub gene in the blue module (Figure 8D). The hub gene from the black module was connected to 56 upregulated DEGs (Figure 8F). The most connected genes were LOC21393691(glycosyltransferase) and LOC21387191(vacuolar-sorting receptor 3). The genes with the largest weight for each module may also be the most important hub genes that respond to different calcium treatments and drought stress in mulberry seedlings.

4. Discussion

Growth and biomass are the most basic indicators of plant growth, and water deficit severely affects both (Barutcular *et al.*, 2016; Anjum et al., 2017). Additionally, based on the above- and below-ground parts, we found that all phenotypes also showed significant changes, suggesting that mulberry plants resisted drought stress by reducing height, diameter, leaf biomass, stem biomass, leaf area, lateral root biomass, total biomass, main root biomass, main root length, lateral root length, root surface area, and root volume in calcium, which promoted these phenotypes. In this study, drought significantly reduced the growth of mulberry seedlings in terms of plant height, ground diameter, and biomass accumulation at all growth stages, which has been reported in many studies (Shang et al., 2019; Zhang et al., 2020a). In this study, instead of alleviating the adverse effects of drought stress, Ca400 treatment aggravated the adverse effects of drought stress. Some researchers have found that drought stress can be alleviated by appropriate concentrations of calcium added to camphor pine seedlings under drought stress, while excessive calcium addition has an antagonistic effect on camphor pine seedlings together with drought stress (Li et al., 2022).

Photosynthesis is the first aspect of plant growth and metabolism to be affected by drought stress (Bulinduo et al., 2010), and drought stress leads to weakened photosynthesis in plants (Liu Shuming et al., 2013). The simultaneous decrease in the net photosynthetic rate, stomatal conductance, and transpiration rate of mulberry seedlings under drought stress suggests that stomatal closure is the main cause of the decrease in stomatal conductance and transpiration rate (Guha et al., 2013), which leads to a decrease in the net photosynthetic rate and inhibition of mulberry seedling growth. In this study, the net photosynthetic rate and stomatal conductance changes were consistent, and the stomatal changes caused by calcium addition were one of the reasons why the net photosynthetic rate of mulberry seedlings first decreased and then increased. In addition, Ca400 had a stronger inhibitory effect on photosynthesis in mulberry seedlings under drought stress, and the addition of higher concentrations of calcium under drought stress may have triggered damage to the photosynthetic apparatus of mulberry seedlings.

Photosynthesis converts light energy into chemical energy, and photosystems I and II are important for executing the photosynthetic light reaction (Zheng et al., 2019). Photosystem I and Photosystem II are oversized pigment-protein complexes that are important for the execution of photosynthetic light reactions (Zheng et al., 2019). In photosystems, the light-harvesting complex (LHC) is the most important component of the photosynthetic light reaction. The light-harvesting complex (LHC) is critical for plants to acquire light energy (Nelson and Yocum, 2006; Shen, 2015). The antenna system consists of two pigment-capturing protein complexes, Lhca and Lhcb, with Lhcb binding to 50 chlorophyll a molecules and being tightly bound to the reaction center. The molecules are tightly bound to the reaction centers to form the peripheral antenna systems CP43 and CP47, which together form the Photosystem II core complex (Najafor). System II core complex (Najafpour et al., 2016; Li, Xingxing, and Hong, Jian, 2018); with the photosystem II core having an interaction with the photosystem II core is the second antenna pigment, the light-trapping pigment complex Lhca, which consists of a 20-30 KDa polypeptide

and binds to chlorophyll a, chlorophyll b, lutein, and carotene (Zhou et al., 2022). In this study, the light-trapping pigment complex II chlorophyll a/b binding protein and PsaL-related genes were downregulated under drought stress, which inhibited the light-trapping of mulberry seedlings. In this study, drought stress inhibited the light-trapping ability and utilization of light energy in the mulberry seedlings, which is consistent with the results of a previous study (Guha et al., 2013).

The phenylpropanoid metabolic pathway is one of the most widely studied secondary metabolic pathways in plants. It consists of a core pathway and multiple branching pathways involving at least 25 enzyme families, producing more than 8000 metabolites, such as coumarins, flavonoids, lignins, phenolic acids, phytoantitoxins, and stilbenes, which are beneficial for plant growth, development, and plant-environment interactions (Gomez-Cano et al., 2020; Dong and Lin, 2021). In general, soil water content can regulate many key genes encoding the main enzymes of phenylpropanoid metabolism, which then stimulate phenylpropanoid biosynthesis in response to drought stress (Clemens and Weber, 2016; Rezayian et al., 2016; Rezayian et al., 2018). Flavonoids act as antioxidants to reduce abiotic stresses, such as drought-induced oxidative damage caused by the accumulation of reactive oxygen species, and they accumulate in large quantities under a certain degree of drought stress (Wang et al., 2022). In this study, Ca400 treatment under drought stress resulted in the upregulation of the phenylpropanoid compounds phenylalanine acid, spermidine, trans-cinnamic acid, erucic acid, erucinol, and pinacoside, and flavonoid synthesis-related genes. This suggests that mulberry seedlings were severely stressed in this environment and that the synthesis of phenylpropanoids increased the resistance of mulberry seedlings. In this study, although drought stress resulted in the downregulation of quercetin and brassinosteroids, a large number of genes related to flavonoid synthesis were upregulated, such as flavonol synthase and flavonoid 3'-monooxygenase bifunctional dihydroflavonol 4-reductase, promoting the synthesis of related flavonoids, which was consistent with the results of previous studies.

This study found that high calcium (Ca400) treatment further suppressed net photosynthetic rate (Pn) and stomatal conductance (Gs) under drought conditions (Figure.2). Transcriptomic data provide a molecular-level explanation for this phenomenon: Ca400-DC treatment specifically led to the downregulation of 20 photosystem I/II antenna protein genes (Lhca/b) and multiple PSI/PSII core subunit genes (Figure. 6). This suggests that high calcium exacerbates drought-induced damage to the photosynthetic apparatus of mulberry seedlings, extending beyond stomatal limitation to include transcriptional suppression of core complexes involved in light energy capture and electron transport, thereby collectively leading to the collapse of photosynthetic capacity.

Plants have developed sophisticated and subtle signaling networks to perceive climate change, induce relative signaling, and activate heat-responsive gene expression during long evolutionary periods. Mining the key genes involved in such molecular processes could facilitate the development of molecular markers, which are necessary to breed heat-tolerant crop species. To uncover the possible molecular processes and key genes contributing to thermotolerance, we conducted WGCNA between genes and metabolites. Two modules were selected based on the correlation values. Six pathways were analyzed: RNA transport, riboflavin metabolism, endocytosis, arachidonic acid metabolism, and glyoxylate and

dicarboxylate metabolism. Glyoxylate and dicarboxylate metabolism are involved in the drought response of mulberry seedlings (Gelaw et al., 2021). KEGG pathway enrichment analysis of DEGs indicated that riboflavin metabolism played a central role in the response of mulberry seedlings to drought stress, and that drought stress significantly inhibited gene expression (Tian et al., 2022). Through WGCNA analysis, we identified seven hub genes highly correlated with stress phenotypes (such as the glycosyltransferase gene LOC21393691 and the vacuolar sorting receptor gene LOC21387191). These genes may occupy central nodes in regulatory networks, responsible for integrating calcium and drought stress signals and regulating downstream photosynthetic and secondary metabolic pathways. For example, LOC21393691 may influence intracellular homeostasis and stress responses by modifying specific metabolites or signaling molecules. This provides key candidate targets for future efforts to elucidate the complex regulatory networks underlying the mulberry tree's adaptation to calcium-drought interactions.

In general, mulberry seedlings may respond to drought stress in a synergistic or antagonistic manner through activated identical or disparate metabolic pathways, depending on the variety, genotype, and frequency and intensity of drought stress.

5. Conclusion

This study investigated the effects of Ca addition on the growth, leaf and root morphology, and biomass accumulation of mulberry seedlings under drought stress and analyzed the photosynthetic physiological response patterns. We also carried out transcriptome and metabolomics analyses and WGCNA, screened differential genes and metabolites, and interpreted the metabolic regulation mechanism of mulberry seedlings in response to drought stress and calcium addition at the histological level. The main conclusions are as follows.

Drought stress significantly inhibited the growth of mulberry seedlings by affecting their growth, biomass accumulation and distribution, leaf morphology, and root morphology. Under drought conditions, high Ca exacerbated the reduction in physiological indices and accelerated the death of mulberry seedlings. Calcium intake is not as good as it should be. Under drought stress, photosynthesis-related genes were downregulated, inhibiting the photosynthetic capacity of the mulberry seedlings. The upregulation of flavonoid synthesis-related genes indicated that the drought tolerance of mulberry seedlings could be improved by promoting the synthesis of flavonoids. WGCNA identified five candidate genes as key regulators of calcium and drought stress. In conclusion, our results provide a new understanding of mulberry seedling responses to drought stress and calcium supplementation, and constitute useful gene resources for forest breeding.

The primary objective of this study is to elucidate the physiological and molecular mechanisms underlying the calcium-drought interaction, rather than to establish guidelines for site selection in afforestation directly. Our conclusions focus more on theoretical insights, such as "deepening our

understanding of how mulberry seedlings adapt to calcium-heterogeneous drought," and do not propose specific recommendations for avoiding certain afforestation sites.

The results indicate that, under specific experimental conditions, the addition of exogenous calcium exacerbates drought stress and accelerates seedling mortality. However, this cannot be directly interpreted to mean that "all calcium-rich soils should be avoided" for afforestation. In actual afforestation practices, there is an optimal range for soil calcium content; levels that are too low or too high may be detrimental to plant growth. One of the values of this study lies in the warning that, in soils that are inherently calcium-deficient or calcium-excessive, blind or excessive calcium supplementation during drought conditions may have adverse effects on plants.

Declarations

Declaration of competing interest

No conflict of interest exists in the submission of this manuscript, and the manuscript is approved by all authors for publication. We declare, on behalf of our co-authors, that the work described is original research.

Author Contribution

Conceptualization: Yongbin Zhou, Chengshu Xin, Liwei Chu. Data curation: Haoyan Liu, Tengzi Zhang, Zhen Wang, Zhi Song. Formal analysis: Haoyan Liu, Tengzi Zhang, Siyu Zuo, Qing Yu. Methodology: Yongbin Zhou, Chengshu Xin, Liwei Chu, Haoyan Liu. Software: Haoyan Liu, Tengzi Zhang, Zhen Wang, Siyu Zuo, Zhi Song. Supervision: Yongbin Zhou, Qingqing Cui, Liwei Chu, Haoyan Liu. Validation: Yongbin Zhou, Tengzi Zhang, Qingqing Cui, Qing Yu, Liwei Chu. Writing original draft: Haoyan Liu, Liwei Chu, Tengzi Zhang.

Data availability statement

Data is provided within the manuscript or supplementary information files.

Funding Statement

This work has no funding support.

References

1. Aaltonen H, Lindén A, Heinonsalo J, Biasi C, Pumpanen J (2016) Effects of prolonged drought stress on Scots pine seedling carbon allocation. Tree Physiol 00: 1-10. https://doi.org/10.1093/treephys/tpw119
2. Anjum SA, Ashraf U, Tanveer M, Khan I, Hussain S, Shahzad B, Zohaib A, Abbas F, Saleem MF, Ali I, Wang LC (2017) Drought induced changes in growth, osmolyte accumulation and antioxidant

metabolism of three maize hybrids. Front Plant Sci 8:69. https://doi. org/10.3389/fpls.. 2017.00069

3. Aras S, Keles H, Bozkurt E (2021) Physiological and histological responses of peach plants grafted onto different rootstocks under calcium deficiency conditions. Sci Hortic 281: 109967. https://doi. org/10.1016/j.scienta.2021.109967
4. Barutcular C, Dizlek H, EL-Sabagh A, Sahin T, Elsabagh M, Islam S (2016) Nutritional quality of maize in response to drought stress during grain-filling stages in Mediterranean climate condition. J Exp Biol Agric Sci 4(6): 644-652. http://dx.doi.org/10.18006/2016.4(Issue6).644.652
5. Chao N, Wang R, Hou C, Yu T, Liu L (2021) Functional characterization of two chalcone isomerase (chi) revealing their responsibility for anthocyanins accumulation in mulberry. Plant Physiol Bioch 161: 65-73. http://dx.doi.org/doi: 10.1016/j.plaphy.2021.01.044
6. Chen K, Li GJ, Bressan RA, Song CP, Zhu JK, Zhao Y (2019) Abscisic acid dynamics, signaling and functions in plants. J Integr Plant Biol 62: 25-54. http://dx.doi.org/doi: 10.1111/jipb.12899
7. Clemens S, Weber M (2016) The essential role of coumarin secretion for Fe acquisition from alkaline soil. Plant Signal Behav 11: e1114197. http://dx.doi.org/doi: 10.1080/15592324.2015.1114197
8. Dong NQ, Lin HX (2021) Contribution of phenylpropanoid metabolism to plant development and plant-environment interactions. J Integr Plant Biol 63: 180-209. http://dx.doi.org/doi: 10.1111/jipb.13054.
9. Dong Q, Wallrad L, Almutairi BO, Kudla J (2022) Ca2+ signaling in plant responses to abiotic stresses. J Integr Plant Biol 64(2): 287-300. http://dx.doi.org/doi: 10.1111/jipb.13228
10. Duursma RA, Kolari M, Permki P, Nikinmaa E, Hari P, Delzon S, Loustau D, Ilvesniemi H, Pumpanen J, Mkel A (2008) Predicting the decline in daily maximum transpiration rate of two pine stands during drought based on constant minimum leaf water potential and plant hydraulic conductance. Tree Physiol 28(2): 265-276. http://dx.doi.org/doi: 10.1093/treephys/28.2.265
11. Ferreira PCG, Hemerly AS (2020) Genome-wide transcriptome profiling provides insights into the responses of maize (Zea mays L.) to diazotrophic bacteria. Plant Soil 451: 121-143. https://doi.org/10.1007/s11104-019-04193-9
12. Gelaw TA, Sanan-Mishra N (2021) Non-Coding RNAs in Response to Drought Stress. Int J Mol Sci 22(22):12519. https://doi: 10.3390/ijms222212519.
13. Głowacka K, Kromdijk J, Kucera K, Xie J, Cavanagh AP, Leonelli L, Leakey ADB, Ort DR, Niyogi KK, Long SP (2018) Photosystem II Subunit S overexpression increases the efficiency of water use in a field-grown crop. Nat Commun 9: 868. https://doi.org/10.1038/s41467-018-03231-x
14. Gomez-Cano L, Gomez-Cano F, Dillon F, Alers-Velazquez R., Doseff AI, Grotewold E, Gray J (2020) Discovery of modules involved in the biosynthesis and regulation of maize phenolic compounds. Plant Sci 291: 110364. https://doi.org/10.1016/j.plantsci.2019.110364
15. Gradowski T, Thomas SC (2008) Responses of Acer saccharum canopy trees and saplings to P, K, and lime additions under high N deposition. Tree Physiol 28: 173-185. https://doi.org/10.1093/treephys/28.2.173

16. Guha A, Sengupta D, Reddy AR (2013) Polyphasic chlorophyll a fluorescence kinetics and leaf protein analyses to track dynamics of photosynthetic performance in mulberry during progressive drought. J Photoch Photobio B 119: 71-83. https://doi.org/10.1016/j.jphotobiol.2012.12.006
17. Guha A, Sengupta D, Reddy AR (2013) Polyphasic chlorophyll a fluorescence kinetics and leaf protein analyses to track dynamics of photosynthetic performance in mulberry during progressive drought. J Photoch Photobio B 119: 71-83. https://doi.org/10.1016/j.jphotobiol.2012.12.006
18. Hammond WM, Williams AP, Abatzoglou JT, Adams HD, Klein T, López R, Sáenz-Romero C, Hartmann H, Breshears DD, Allen CD (2022) Global field observations of tree die-off reveal hotter drought fingerprint for Earth's forests. Nat Commun 13: 1761. https://doi.org/10.1038/s41467-022-29289-2
19. Hardoim PR, de Carvalho TLG, Ballesteros HGF, Bellieny RD, Rojas CA, Venancio TM, Hartmann HM, Moura CF, Anderegg, William RLA, Ruehr, NK, Salmon Y, Allen, CD, Arndt, SK, Breshears DD, Davi H, Galbraith D, Ruthrof KX, Wunder J, Adams HD, Bloemen J, Cailleret M, Cobb R, Gessler A, Grams TEE, Jansen S, Kautz M, Lloret F, O'Brien M (2018) Research frontiers for improving our understanding of drought-induced tree and forest mortality. New Phytol 218: 15-28. https://doi.org/10.1111/nph.15048
20. Hatfield, JL, Prueger, JH (2015) Temperature extremes: Effect on plant growth and development. Weather Clim Extrem, 10, 4–10. https://doi.org/10.1016/j.wace.2015.08.001
21. He N J, Zhao A C, Qin J, Zeng Q W, Xiang Z H (2012) The Mulberry Genome Project and the Mulberry Industry. Seri. Sci, 38(1): 0140-0145. https://doi.org/10.13441/j.cnki.cykx.2012.01.026
22. Hu H, Liu Y, He B, Chen X, Ma L, Luo Y, Fei X., Wei A (2022) Integrative physiological, transcriptome, and metabolome analysis uncovers the drought responses of two Zanthoxylum bungeanum cultivars. Ind Crop Prod 189: 115812. https://doi.org/10.1016/j.indcrop.2022.115812
23. Ji Feiteng, Li Nan, Deng Xin (2009) Characteristics of calcium content in plants in Karst region and analysis of high calcium adaptation modes. J Plant Ecol 33(5):926-935. https://doi.org/10.5194/bg-15-2991-2018
24. Jing DW, Xing SJ, Du ZY, Liu FC (2013) Effects of drought stress on growth, photosynthetic characteristics, and reactive oxygen species metabolism of poplar seedlings. J Appl Ecol 24(7): 1809-1816. Chinese. PMID: 24175508.
25. Kang J, Zhao W, Zheng Y, Zhang D, Zhou H, Sun P (2017) Calcium chloride improves photosynthesis and water status in the C4 succulent xerophyte Haloxylon ammodendron under water deficit. Plant Growth Regul 82: 467-478. https://doi.org/10.1007/s10725-017-0273-4
26. Li H, Huo Y, Weng X, Zhou Y, Sun Y, Zhang G, Zhang S, Liu L, Pei J (2022) Regulation of the growth of Mongolian pine (Pinus sylvestris var. mongolica) by calcium-water coupling in a semiarid region. Ecol Indic 137: 108736. https://doi.org/10.1016/j.ecolind.2022.108736
27. Li Qiang, Cao J H, Yu LJ, Chestnut M T, Liao J J, Gan Lu (2010) Effects of exogenous calcium on photosynthetic physiology of Lonicera japonica during drought stress. J Ecol Environ 19(10): 2291-2296. https://doi.org /10.3316/informit.007647760420872

28. Li Y, Zhang T, Zhou Y, Zou X, Yin Y, Li H, Liu L, Zhang S (2021) Ectomycorrhizal symbioses increase soil calcium availability and water use efficiency of Quercus acutissima seedlings under drought stress. Eur J Forest Res 140(5): 1039-1048. https://doi.org/10.1007/s10342-021-01383-y
29. Li, Mingxing, and Hong, Jian (2018) Advances in the study of plant photosystem proteins. Comput Biol 8(1): 1-7. https://doi.org/10.1042/BST20170307
30. Liu C, Hu J, Fan W, Zhu P, Cao B, Zheng S, Xia Z, Zhu Y, Zhao A (2021) Heterotrimeric G-protein γ subunits regulate ABA signaling in response to drought through interacting with PP2Cs and SnRK2s in mulberry (Morus alba L.). Plant Physiol Biochem 161: 210-221. https://doi.org/10.1016/j.plaphy.2021.02.017
31. Liu L, Cao X, Zhai Z, Ma S, Tian Y, Cheng J (2022) Direct evidence of drought stress memory in mulberry from a physiological perspective: Antioxidative, osmotic and phytohormonal regulations. Plant Physiol Biochem 186: 76-87. https://doi.org/ 10.1016/j.plaphy.2022.07.001
32. Liu Shuming, Sun Jiaqian, Deng Zhenyi, Wei Diandian, Zhang Gang, Sun Bingyin (2013) Effects of drought stress on root growth and water utilisation of different pepper varieties. Forest Sci 49(12): 30-35.
33. Murray V, Ebi KL (2012) IPCC special report on managing the risks of extreme events and disasters to advance climate change adaptation (SREX). J Epidemiol Commun H 66: 759-760. 9781107607804 (paperback) www.cambridge.org/9781107607804
34. Najafpour MM, Renger G, Hołyńska M, Moghaddam AN, Aro E-M, Carpentier R, Nishihara H, Eaton-Rye JJ, Shen J-R, Allakhverdiev SI (2016) Manganese Compounds as Water-Oxidizing Catalysts: From the Natural Water-Oxidizing Complex to Nanosized Manganese Oxide Structures. Chem Rev 116: 2886-2936. https://doi.org/10.1021/acs.chemrev.5b00340
35. Nelson N, Yocum CF (2006) Structure and Function of Photosystems I and II. Annu Rev Plant Biol 57: 521-565. https://doi.org/10.1146/annurev.arplant.57.032905.105350
36. O'Leary B, Plaxton WC (2020) Multifaceted functions of post-translational enzyme modifications in the control of plant glycolysis. Current Opinion in Plant Biology 55: 28-37. https://doi.org/10.1016/j.pbi.2020.01.009.
37. Pan Y, Chai X, Gao Q, Zhou L, Zhang S, Li L, Luan S (2019) Dynamic interactions of plant CNGC subunits and calmodulins drive oscillatory Ca^{2+} channel activities. Dev Cell 48: 1-16 https://doi.org/10.1016/j.devcel.2018.12.025
38. Peres ALGL, Soares JS, Tavares RG, Righetto G, Zullo MAT, Mandava NB, Menossi M (2019) Brassinosteroids, the sixth class of phytohormones: a molecular view from the discovery to hormonal interactions in plant development and stress adaptation. Int J Mol Sci 20: 331. https://doi.org/10.3390/ijms20020331
39. Rezayian M, Niknam V, Ebrahimzadeh H (2018) Differential responses of phenolic compounds of Brassica napus under drought stress. J Plant Physiol 8(3): 2417-2425. https://doi.org/10.22034/IJPP.2018.540887

40. Rohela GK, Muttanna PS, Kumar R, Chowdhury SR (2020b) Mulberry (Morus spp.): an ideal plant for sustainable development. Trees Forests People 2: 100011. https://doi.org/10.1016/j.tfp.2020.100011
41. Rohela GK, Phanikanth J, Mir MY, Aftab AS, Pawan S, Sadanandam A, Kamili AN, (2020a) Indirect regeneration and genetic fidelity analysis of acclimated plantlets through SCoT and ISSR markers in *Morus alba* L. cv. Chinese white. Biotechnol Rep 25: 313-321. https://doi.org/10.1016/j.btre.2020.e00417
42. Shang Y (2019) Effects of elevated ozone and water deficit on poplar saplings: Changes in carbon and nitrogen stocks and their allocation to different organs. Forest Ecol Manag 441: 89-98. https://doi.org/10.1016/j.foreco.2019.03.042
43. Shen JR (2015) The structure of photosystem II and the mechanism of water oxidation in photosynthesis. Annu Rev Plant Biol 66: 23-48. https://doi.org/10.1146/annurev-arplant-050312-120129
44. Simón BFD, Sanz M, Sánchez-Gómez D, Cadahía E, Aranda, I (2020) Rising [CO2] effect on leaf drought-induced metabolome in Pinus pinaster Aiton: ontogenetic- and genotypic-specific response exhibit different metabolic strategies. Plant Physiol Bioch 149: 201-216. https://doi.org/10.1016/j.plaphy.2020.02.011
45. Steinhorst L, Kudla J (2013) Calcium-a central regulator of pollen germination and tube growth. Bioch Biophy Acta 1833: 1573-1581. https://doi.org/10.1016/j.bbamcr.2012.10.009
46. Tian Q, Wang G, Ma X, Shen Q, Ding M, Yang X, Luo X, Li R, Wang Z, Wang X, Fu Z, Yang Q, Tang J, Wang G (2022) Riboflavin integrates cellular energetics and cell cycle to regulate maize seed development. Plant Biotechnol J Aug;20(8):1487-1501. https://doi.org/ 10.1111/pbi.13826.
47. Wang D, Sun C, Cui M, Shen X, Zhang Y, Xiao J, Liu P, Zhang Y, Xie H (2022) An integrated analysis of transcriptome and metabolome provides insights into the responses of maize (Zea mays L.) roots to different straw and fertilizer conditions. Environ exp bot 194: 104732. https://doi.org/10.1016/j.envexpbot.2021.104732
48. Weng X, Li H, Ren C, Zhou Y, Zhu W, Zhang S, Liu L (2022) Calcium Regulates Growth and Nutrient Absorption in Poplar Seedlings. Front Plant Sci https://doi.org/10.3389/fpls.2022.887098
49. Williams PA, Allen CD, Macalady AK, Griffin D, Woodhouse CA, Meko DM, Swetnam TW, Rauscher SA, Seager R, Grissino-Mayer HD, Dean JS, Cook ER, Gangodagamage C, Cai M, McDowell NG (2013) Temperature as a potent driver of regional forest drought stress and tree mortality. Nat Clim Change 3(3): 292-297. https://doi.org/10.1038/nclimate1693
50. Xu CG, McDowell NG, Fisher RA, Wei L, Sevanto S, Christoffersen BO, Weng ES, Middleton RS (2019) Increasing impacts of extreme droughts on vegetation productivity under climate change. Nat Clim Change 9: 948-953. https://doi.org/10.1038/s41558-019-0630-6
51. Yang B, Cui Q, Meng Y, Zhang Z, Hong Z, Hu F, Li J, Tao C, Wang Z, Zhang W (2023) Combined multivariate drought index for drought assessment in China from 2003 to 2020. Ag Water Manage, 281: 108241. https://doi.org/10.1016/j.agwat.2023.108241

52. Yu R, Zhai P (2020) Changes in compound drought and hot extreme events in summer overpopulated eastern China. Weather and Clim Extreme 30: 100295. https://doi.org/10.1016/j.wace.2020.100295
53. Zeb Q, Wang X, Hou C, Zhang X, Dong M, Zhang S, Zhang Q, Ren Z, Tian W, Zhu H, Li L, Liu L (2020) The interaction of CaM7 and CNGC14 regulates root hair growth in Arabidopsis. J Integr Plant Biol 62: 887-896. https://doi.org/10.1111/jipb.12890
54. Zhang H, Li X, Xu Z, Wang Y, Sun G (2020b) Toxic effects of heavy metals Pb and Cd on mulberry (Morus alba L.) seedling leaves: Photosynthetic function and reactive oxygen species (ROS) metabolism responses. Ecotox Environ Safe 195: 110469. https://doi.org/10.1016/j.ecoenv.2020.110469
55. Zhang HH, Xu N, Teng ZY, Wang JR, Ma SL, Wu XY, Li X, Sun GY (2019) 2-Cys Prx plays a critical role in scavenging H2O2 and protecting photosynthetic function in leaves of tobacco seedlings under drought stress. J Plant Interact 14: 119-128. https://doi.org/10.1080/17429145.2018.1562111
56. Zhang Huihui, Zhang Xiuli, Xu Nan, He Guoqiang, Jin Weiwei, Yue Bingbing, Li Xin, Sun Guangyu (2011) Effects of exogenous calcium on the function of photosystem II in tobacco seedlings under drought stress. J Appl Ecol 22(5): 1195-1220. Chinese. PMID: 21812294.
57. Zhang Z, Tariq A, Zeng F, Graciano C, Zhang B (2020a) Nitrogen application mitigates droughtinduced metabolic changes in Alhagi sparsifolia seedlings by regulating nutrient and biomass allocation patterns. Plant Physiol Bioch 155: 828-841. https://doi.org/10.1016/j.plaphy.2020.08.036
58. Zheng L, Li Y, Li X, Zhong Q, Li N, Zhang K, Zhang Y, Chu H, Ma C, Li G, Zhao J, Gao N (2019) Structural and functional insights into the tetrameric photosystem I from heterocyst-forming cyanobacteria. Nat Plants 5(10): 1087-1097. https://doi.org/10.1038/s41477-019-0525-6
59. Zhou Y, Liu Z, Yao M, Chen J, Xiao Y, Han G, Shen JR, Wang F (2022) Elucidating the Molecular Mechanism of Dynamic Photodamage of Photosystem II Membrane Protein Complex by Integrated Proteomics Strategy. CCS Chemistry 4: 182-193. https://doi.org/10.31635/ccschem.021.202000583

Figures

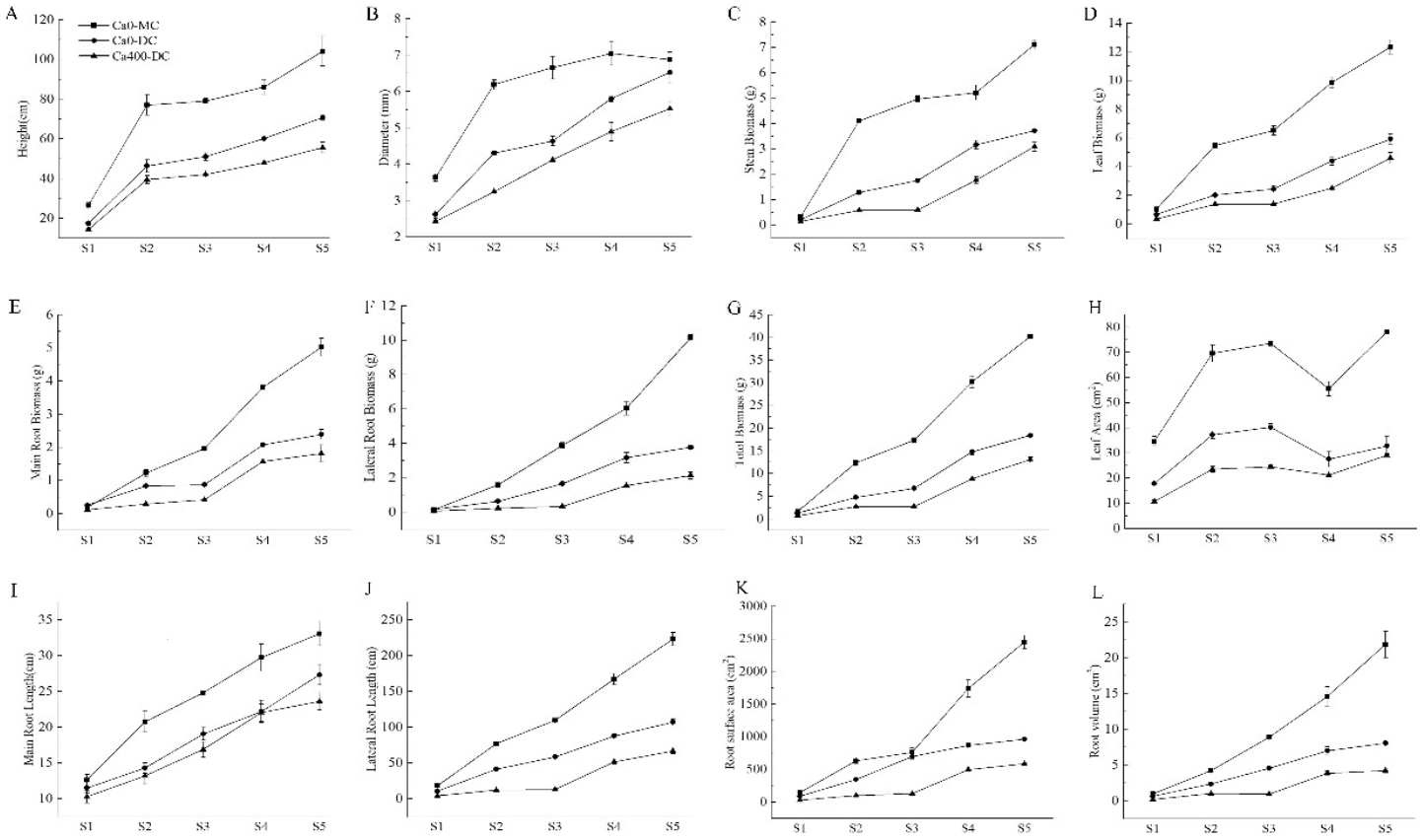


Figure 1

Effects of Ca addition on growth and leaf morphology of mulberry seedlings under drought stress (A) Height (B) Diameter (C) Leaf biomass (D) Stem biomass (E) Main root biomass (F) Lateral root biomass (G) Total biomass (H) Leaf area (I)Main root length (J) Lateral root length (K) Root surface area (L) Root volume

The square is Ca0-MC, the circle is Ca0-DC, and the triangle is Ca400-DC.

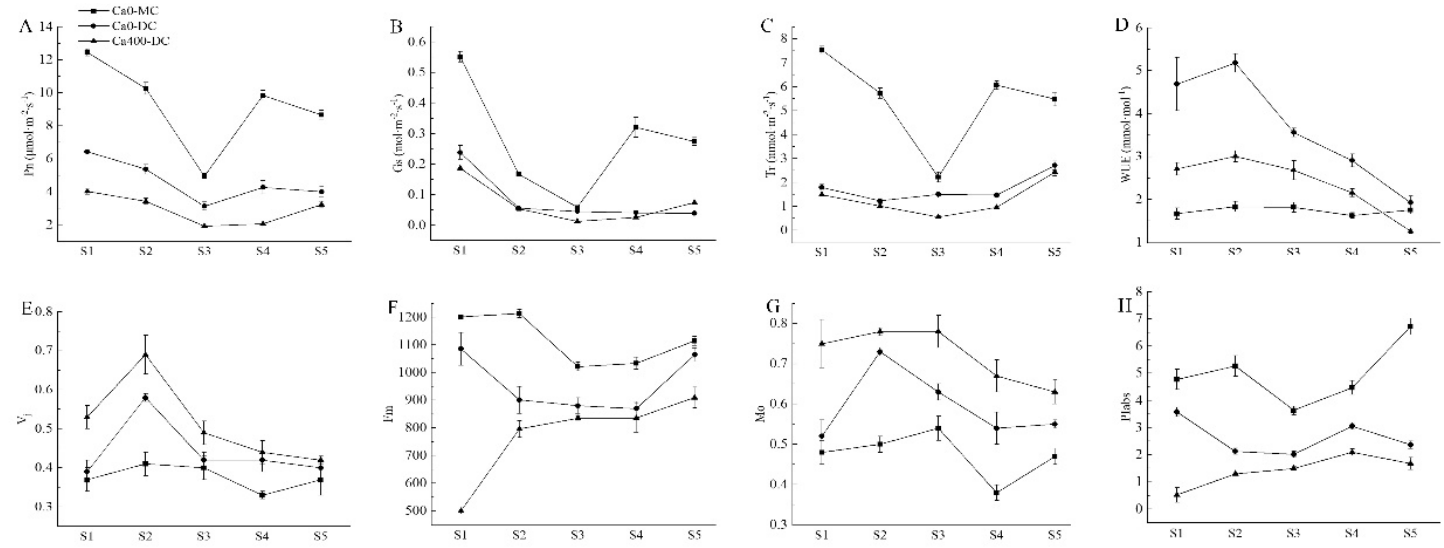


Figure 2

Effects of Ca addition on photosynthetic parameters and fluorescence parameters of mulberry seedlings under drought stress from S1 to S5 (A) Pn (B) Gs (C) Tr (D) WUE (E) VJ (F) FM (G) MO (H) PIabs



Figure 3

Fluorescence parameters radar plot of Ca addition under drought stress from S1 to S5 (A) S1 (B) S2 (C) S3 (D) S4 (E) S5

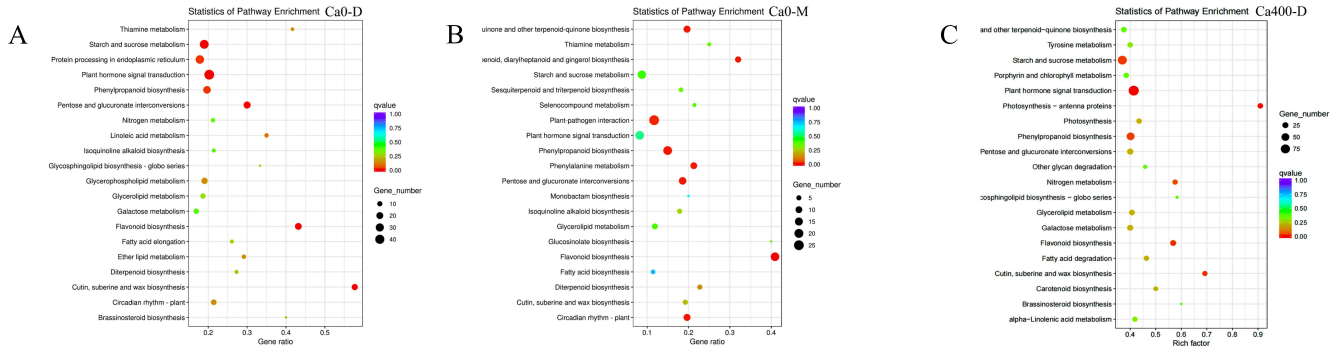


Figure 4

Enrichment and classification analysis of DEGs, (A) KEGG enrichment analysis of Ca0-DC, (B) KEGG enrichment analysis of Ca0-MC, and (C) KEGG enrichment analysis of Ca400-DC.

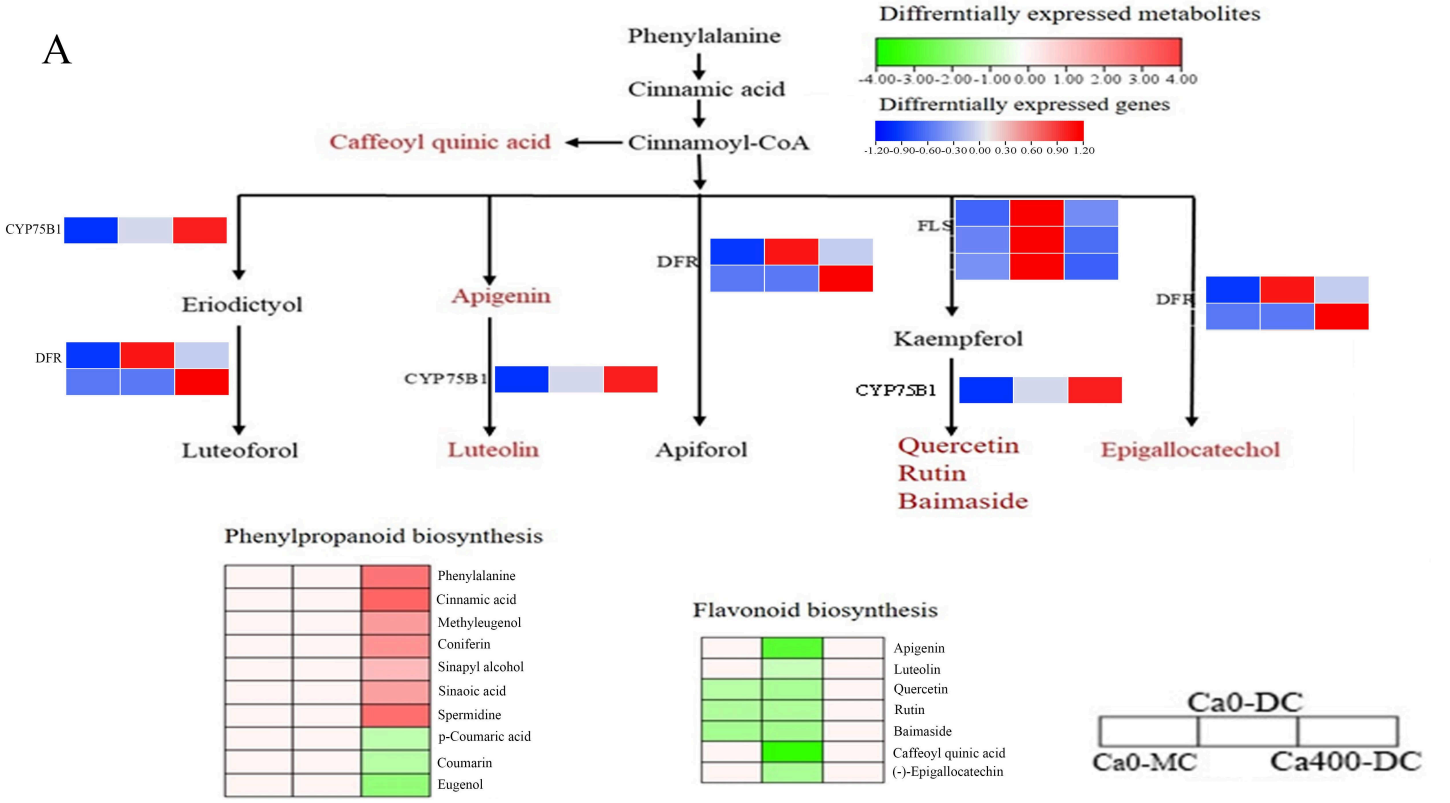


Figure 5

Schematic representation of the association analysis (A) phenylpropanoids biosynthesis

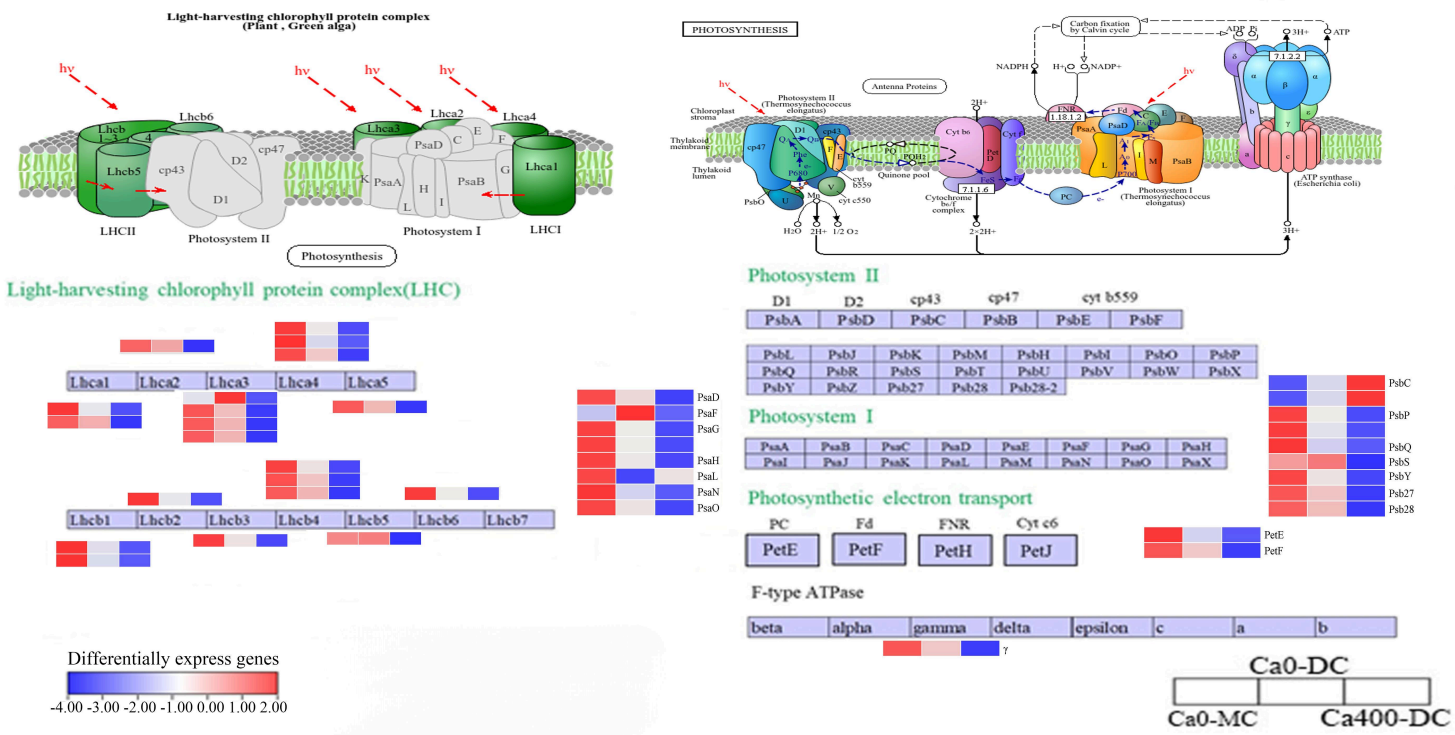


Figure 6

Schematic representation of the association analysis of the photosynthesis pathway

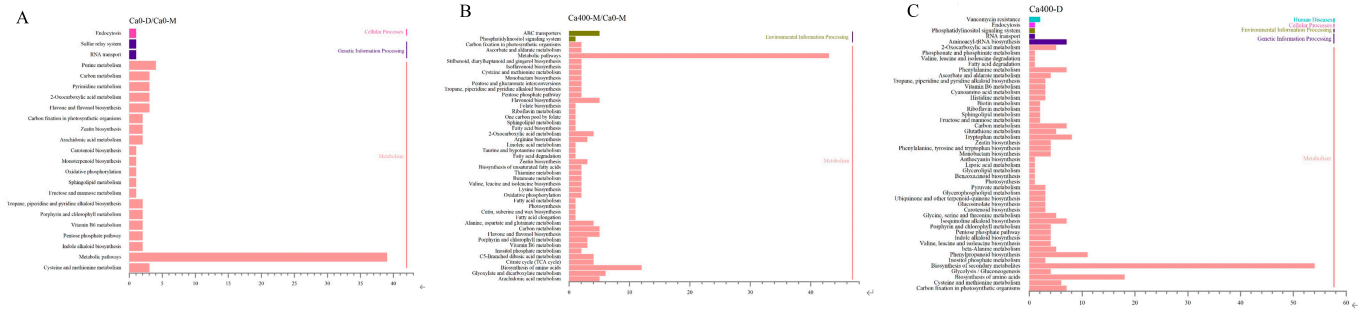


Figure 7

(A) DEMs analysis of Ca0-DC, (B) DEMs classification analysis of Ca0-MC, (C) DEMs classification analysis of Ca400-DC

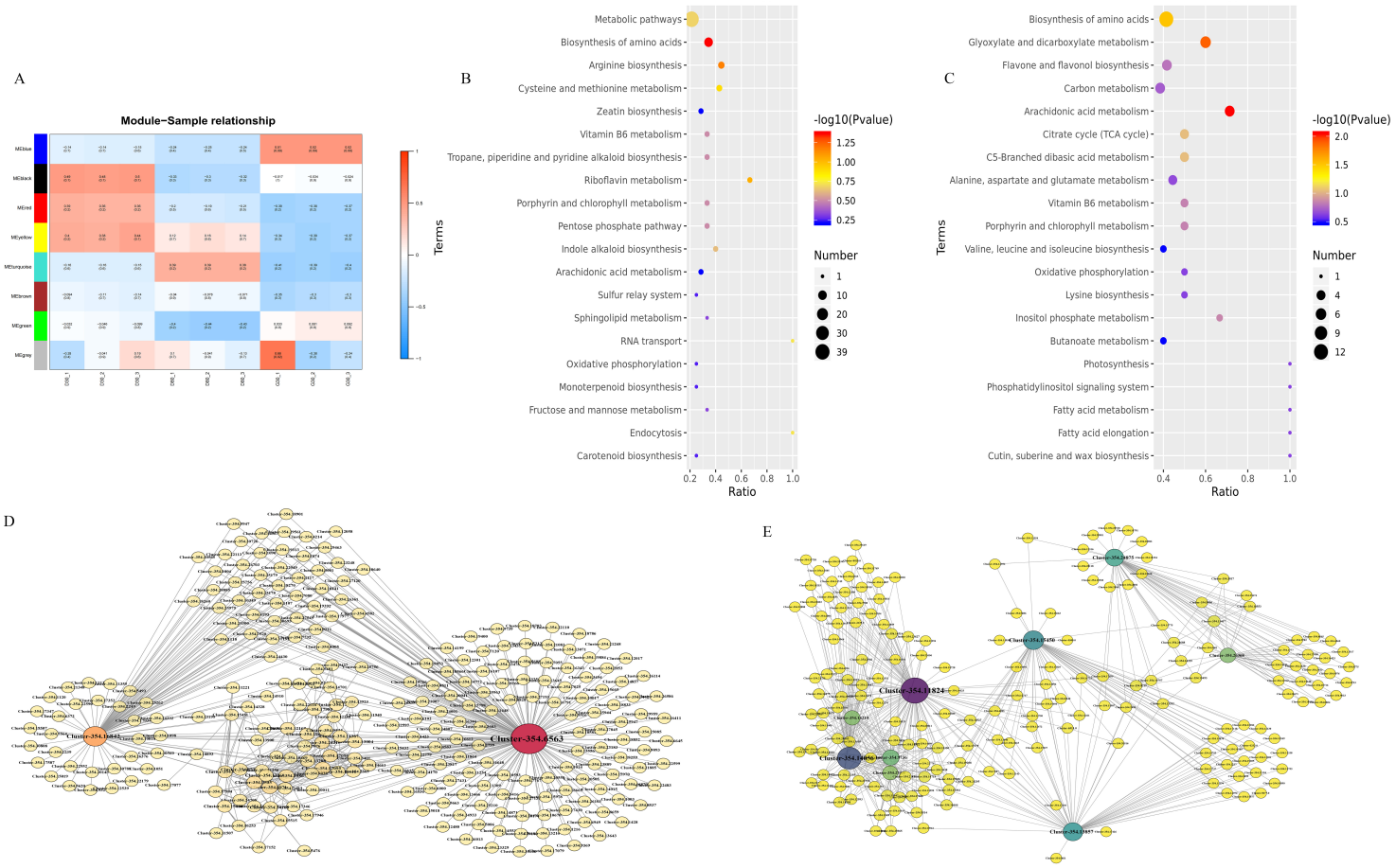


Figure 8

Correlation analysis of key pathways and hub genes involved in different calcium treatments and drought stress response in mulberry seedlings. Spearman correlation analysis of metabolic pathways and DEGs. The squares with different colors in the first column represent different modules (A). KEGG enrichment analysis of blue(B) and black(C). Hub genes identified in the blue (D) and black (E) modules. Log2FC of each connected gene is shown by the thickness of the lines and the size of the circles; the degree between the hub gene and connected genes is indicated by the color intensity of the circle. The most connected genes are marked.

Supplementary Files

This is a list of supplementary files associated with this preprint. Click to download.

- SupplementaryFigure1.jpg
- SupplementaryFigure2.jpg
- SupplementaryFigure3.jpg
- SupplementaryFigure4.jpg

- SupplementaryFigure5.jpg
- SupplementaryFigure6.jpg
- SupplementaryFigure7.jpg